

Received October 20, 2020, accepted November 1, 2020, date of publication November 17, 2020, date of current version December 7, 2020.

Digital Object Identifier 10.1109/ACCESS.2020.3038807

Prefrontal Brain Electrical Activity and Cognitive Load Analysis Using a Non-linear and Non-Stationary Approach

CHIH-SUNG CHEN^{1,3}, TSUNG-H-SIN CHIEN^{1,2}, PO-LEI LEE^{ID 3}, (Member, IEEE),
YIH JENG¹, (Member, IEEE), AND TING-KUANG YEH^{ID 1,2}

¹Department of Earth Sciences, National Taiwan Normal University, Taipei City 106, Taiwan, R.O.C.

²Institute of Marine Environmental Science and Technology, National Taiwan Normal University, Taipei City 106, Taiwan, R.O.C.

³Department of Electrical Engineering, National Central University, Taoyuan City 32001, Taiwan, R.O.C.

Corresponding authors: Yih Jeng (geofv001@ntnu.edu.tw) and Ting-Kuang Yeh (tkyeh@ntnu.edu.tw)

This work was supported in part by the Ministry of Science and Technology, Taiwan, R.O.C., under Grant MOST 108-2634-F-008-003, Grant MOST 107-2511-H-003-010-MY3, and Grant MOST 107-2634-F-008-003; and in part by the Institute for Research Excellence in Learning Sciences of the National Taiwan Normal University from the Featured Areas Research Center Program within the framework of the Higher Education Sprout Project of the Ministry of Education, Taiwan, R.O.C.

ABSTRACT This study presents an instantaneous spectrum analysis for electroencephalograph data processing that would facilitate the practice of learning and instruction through real-time measurements of the learner's cognitive load. The instantaneous spectrum analysis is derived from the ensemble empirical mode decomposition which decomposes signals into a gathering of intrinsic mode functions without mode mixing. The multi-marginal Hilbert-Huang spectrum is introduced to estimate frequency contents. As a result, the amplitude of brain rhythms related to the cognitive load can be determined accurately. A model study was performed at first to test the efficacy of the proposed algorithm by comparing with the Fourier based technique, then a prefrontal experiment was conducted to show the advantages of the proposed method. With the higher resolution and more realistic of the proposed method relative to conventional spectrum analysis, more significant features of the signal can be extracted. We believe that the proposed method has the potential to be a substantial technique in electroencephalograph data analysis.

INDEX TERMS Electroencephalograph, cognitive load, ensemble empirical mode decomposition, multi-marginal Hilbert-Huang spectrum, brain rhythms.

I. INTRODUCTION

Cognitive load is essential for understanding instructional design quality and optimizing working memory capacity on learning during instruction [1]. Several innovative processes and methodologies based on physiological measures for analyzing cognitive load are available [2]–[6]. Dan and Reiner [7] indicated that observing psycho-physiological changes when they occur in response to the progression of a learning session allows for adjusting the individual learner's capabilities. This observation usually can be achieved by detecting the brain's electrical activities. Electroencephalograph (EEG) is a non-invasive electrophysiological monitoring device to detect electrical activities of the brain [8]. The

The associate editor coordinating the review of this manuscript and approving it for publication was Junhua Li^{ID}.

accessibility of the EEG device and advanced near-real-time analysis techniques have improved the quality of teaching and learning in various aspects [3], [4], [7]. Nowadays, the EEG is also an effective tool in the study of machine learning, such as providing new communication and control options for individuals to interact with the external world [9] or monitoring human driving behavior to reduce traffic accidents [10].

It is well documented that when the brain performs a working memory task, the frontal/prefrontal cortex makes a change in energy transfer in the brain due to the activity of working memory [11]–[14]. At least five distinct rhythms (waves) of electrical activity in the brain have been reported [15]–[18]. Among those waves, Alpha (8~14 Hz) and Theta (4~8 Hz) are two of these waves sensitive to cognitive, comprehending, and working memory performance [17], [19], [20].

Most studies regarding the brain's electrical activity and cognitive load are focused on the frontal cortex, and prefrontal data are rare. The standard methods used for processing the data are Fourier based spectrum analysis [21], [22]. In recent years, some novel techniques were proposed for EEG data analysis, including wavelet transforms [23]–[26] and empirical mode decomposition (EMD) based methods [27]–[30].

From the viewpoint of instruction efficacy, numerous studies show that an appropriate instructional method reduces the cognitive load in learners, and efficiently uses the working memory capacity; however, the individual cognitive load varies according to the demands of the task with time [31]–[33]. Consequently, reliable and accurate measurement of cognitive load with EEG is crucial in developing successful instructional methods.

There are many advantages of using EEG in studying brain activities such as the possibility of measuring modulations of electric potentials over time [34], providing qualitative information about neural activities [35], and achieving high temporal resolution of the signal [36]. However, it has some limitations that we should pay attention to, which are low spatial resolution, susceptible to motion artifacts, and difficulty in estimating workload precisely [4], [26]. The precise measurement of cognitive load using EEG signals is still under research, particularly to investigate the prefrontal EEG signals classification across different cognitive tasks levels.

Our study aims to develop a novel non-linear and non-stationary data processing scheme to upgrade EEG data measurement and interpretation precision. To this end, an arithmetic task with four levels of difficulty was designed to examine the electrical activities of the prefrontal cortex at different difficulty levels. The proposed method is mainly derived from the ensemble empirical mode decomposition (EEMD) instantaneous attributes [37], [38], which includes the computation of amplitude, phase, and frequency at any given time. Once a meaningful time-frequency-amplitude distribution (spectrogram) is obtained, the multi-marginal Hilbert-Huang spectrum (MHHS), an extension of the marginal Hilbert spectrum [39], [40], can be evaluated accordingly to determine the participants' cognitive load. The proposed method is demonstrated in a model study and then compared with the conventional Fourier-based technique with real data to validate our findings.

II. OVERVIEW OF SUBJECTS AND EXPERIMENT

A mental arithmetic assessment was designed for the experiment. To avoid bias and to reduce false data, a standard inspection for cognitive load EEG subjects was carried out before conducting the experiment. The educational background, age, and health condition of all subjects must be compatible, but the experiment was not gender-classified. Also, all the subjects were required not to have been involved in any mental arithmetic training. With the above requirements, we recruited 20 subjects. All of the subjects were college students between 20 and 25 years old, physically and

mentally healthy, and having no history of any brain disease or mental illness. All subjects were asked to take four mental arithmetic tasks of different difficulty levels:

- (1) Two-digit by one-digit multiplication problem with single-digit carry only. For example: 72×3 , 81×9 , and 61×7 .
- (2) Two-digit by one-digit multiplication problem with ones and tens digits carries. For example: 32×7 , 45×5 , and 18×9 .
- (3) Three-digit by one-digit multiplication problem with tens and hundreds digits carries. For example: 431×5 , 393×3 , and 621×7 .
- (4) Three-digit by one-digit multiplication problem with ones, tens, and hundreds digits carries. For example: 956×2 , 684×4 , and 527×5 .

Twenty-five questions on each level of the mental arithmetic task were designed according to the cognitive load and working memory capacity. The difficulty levels were distinguished by the complexity of calculation, as listed above. Subjects were instructed to mentally solve all questions of the easiest level and then finish questions in the next level of difficulty. This running order is consistent with the procedure for evaluating working memory adopted in the Wechsler Memory Scale (WMS-III) [41] which is the most thoroughly standardized instruments for the neuropsychological assessment of memory. There was no specific individual design for calculation complexity of each question on the same level. The multiplier and multiplicand of each question on the same level were randomly selected from among integers with the predefined number of digits. We avoided any leading or misleading questions. All the questions were neutral and unbiased; this is evident that the responding Theta amplitudes of the 25 questions on the same difficulty level show no significant trend (Fig. 5 in RESULTS). There was no time limit for answering the questions, but subjects were asked to answer each question as soon as possible.

III. METHODS

The EEG signal is generated from the brain's electrical activity that is a non-linear and non-stationary process. In such a case, the frequency of the data should be ever-changing, and having an instantaneous attribute. The EEG signal analysis by applying techniques like the fast Fourier transform (FFT), short-time Fourier transform, spectral EEG features, wavelet, or standard Hilbert transform are effective [22]–[26], however, the problems of time and frequency resolution and end-effects should be considered [40], [42]. Therefore, we introduce the EEMD spectrogram using the marginal Hilbert spectrum to analyze EEG data. This section is a brief description of the proposed method.

A. DATA DECOMPOSITION

The first step of analyzing the acquired EEG data is to perform data decomposition to determine the feature of the data and extract meaningful components to build up the

base for spectrogram analysis. We adopt an empirically based adaptive data-analysis method initially proposed by Huang, *et al.* [40] called EMD, and it was upgraded to an advanced version EEMD by Wu and Huang [38]. The EEMD method is intuitive, direct, and adaptive with an *a posteriori*-defined basis [38], [40]. This method presumes that any data are composed of a series of simple oscillatory modes of different frequency bands called intrinsic mode functions (IMFs) which fulfill the following two conditions: (1) the number of minima, maxima, and the number of zero crossings must be equal, or differ by one at most; (2) the envelopes determined by the local maxima and that by the local minima are symmetrical to zero [40]. Any data can be decomposed through the sifting process [37], [40].

Unlike the mono-frequency and stationary harmonics as assumed in the Fourier analysis, the IMFs contain time-variable amplitudes and frequencies which are corresponding to the physical properties of the data. Through the sifting procedure of the EMD/EEMD decomposition, the data can be decomposed into a set of IMFs and a residue, a monotonic function or a function from which no more IMF can be extracted [37], [40]. If the data contain non-IMF components, those will be in the residue. The decomposition result is expressed by a simple equation:

$$x(t) = \sum_{j=1}^n c_j(t) + r_n(t) \quad (1)$$

where j denotes the number of IMFs, $c_j(t)$ is the j -th IMF, and $r_n(t)$ is the final part interpreted as the DC component or residual of $x(t)$ after n -times sifting. The number n , an integer within the range between 1 and a finite integer, indicates the number of sifting or the total number of IMFs. It has been shown that the total number of IMFs of a data set is close to $\log_2 N$ where N is the number of total data points [43]. In practice, the number of IMFs depends on the sifting stoppage criteria achieved by a Cauchy type of convergence test [38], [40]. The more rigorous the stoppage criterion is set, the more IMFs are obtained. However, too many IMFs are not suggested because it could make the resulting IMFs approaching harmonic functions lacking physical meaning [44]. More details regarding the decomposition method can be found in various publications [40], [43], [45]–[47]. Here we target the discussion on the concepts of instantaneous frequency attribute and marginal Hilbert spectrum, which are used in processing the EEG data.

B. INSTANTANEOUS FREQUENCY

The computation of instantaneous frequency is straight forward in conventional Hilbert transform by finding the complex conjugate pair $x(t)$ and $y(t)$, where $y(t)$ is the Hilbert transform of data $x(t)$. Mathematically, it can be expressed as

$$y(t) = \frac{1}{\pi} P \int_{-\infty}^{\infty} \frac{x(\tau)}{t - \tau} d\tau \quad (2)$$

$$x(t) = -\frac{1}{\pi} P \int_{-\infty}^{\infty} \frac{y(\tau)}{t - \tau} d\tau \quad (3)$$

[48]–[50] where P is the Cauchy principal value of the integral. With the complex conjugate available, we then have the complex trace $z(t)$

$$z(t) = x(t) + iy(t) = a(t)e^{i\vartheta(t)} \quad (4)$$

where $a(t)$ denotes the instantaneous amplitude (envelope amplitude) or simply called envelope by some investigators, and $\vartheta(t) = \tan^{-1}(y(t)/x(t))$ (rotation angle) is the instantaneous phase. The instantaneous frequency $\Omega(t)$ then can be easily defined mathematically as

$$\Omega(t) = \frac{d\vartheta(t)}{dt} \quad (5)$$

The above derivation is the so-called analytic signal method, which computes the instantaneous frequency through the conventional Hilbert transform. Although the analytic signal method is mathematically compact and effective, there are some difficulties in computation that have been arguing among many investigators [51]–[54]. The major controversy is that the function must be mono-component and have a non-overlapping spectrum to produce a physically meaningful instantaneous frequency [48], [53]. Huang *et al.* [55] gave an example to describe the difficulties of computing instantaneous frequency, and Chen and Jeng [37] followed a similar derivation. Both results confirmed that the instantaneous frequency exists only if the input signal is a mono-component function with zero mean symmetry at any given time.

Huang *et al.* [55] introduced efficient EMD based algorithms, the normalized Hilbert transform and the direct quadrature, to remedy deficiencies of the analytic signal instantaneous frequency computation. However, some difficulties are still unsolved, e.g. the amplitude modulation (AM) part of the data is ignored, and the IMFs are mode mixed. Chen and Jeng [37] proposed a more rigid method to derive the instantaneous attributes by incorporating the EEMD into their algorithm, which overcomes the mode mixing problems and reduces the artificial fluctuations.

C. NLT EEMD ALGORITHM

The EMD algorithm has shortcomings of mode mixing, stoppage criterion, and false end effect, which impede to obtain accurate computation of instantaneous frequency. Wu and Huang [38] proposed a noise assisted method, EEMD, to alleviate these difficulties. Chen and Jeng [37] introduced a complete algorithm, the natural logarithm transformed (NLT) EEMD, to improve the signal/noise ratio of ground-penetrating radar data. The method that we apply to compute the spectrogram of EEG data integrates two algorithms [37], [56] proposed by Chen and Jeng, which is briefly described below:

1. Take the NLT of the data if the data are seriously attenuated. The transform function is defined as,

$$L(t) = \text{sign}[c \log(a + |x(t)|)]$$

$$\text{sign} = \begin{cases} 1, x(t) > 0 \\ 0, x(t) = 0 \\ -1, x(t) < 0 \end{cases} \quad (6)$$

where $L(t)$ is the logarithm of the data $x(t)$; the sign function is used to keep the original data polarity; the constant a is a value to avoid negative logarithmic value; the scaling constant c is the control of maximum output value.

2. Add a white noise series $w(t)$ to the data $x(t)$ or attenuation-compensated data $L(t)$. The white noise should have scales populated uniformly through the whole time-frequency space. For simplicity, we use the data without NLT:

$$X(t) = x(t) + w(t) \times R \quad (7)$$

where R is the ratio of the amplitude standard deviation of $w(t)$ to that of the $x(t)$.

3. Derive IMFs from the white noise added data $X(t)$ by using the EMD algorithm.

$$X(t) = \sum_{j=1}^n C_j(t) + R_n(t) \quad (8)$$

4. Repeat steps 2 and 3 with sufficient times m ; each time different white noise of the same amplitude is added to obtain an ensemble G_j of the corresponding j^{th} IMF and residue

$$G_j(t) = \sum_{l=1}^m C_{jl} \quad (9)$$

where j is the j^{th} level of IMF; l is the index of ensemble members, and m is called the number of ensemble members.

5. Calculate the ensemble mean on each level of IMFs

$$\bar{C}_j(t) = \frac{G_j(t)}{m} = \frac{1}{m} \sum_{l=1}^m C_{jl} \quad (10)$$

6. Derive the instantaneous frequency and perform the fluctuation control.

- i) Remove local fluctuations: If $f(t_i)$, the instantaneous frequency of a data point in the time domain, is greater than one standard deviation, it will be replaced by the mean of neighboring two data point values $f(t_{i-1})$ and $f(t_{i+1})$.
- ii) Reduce end effect: Slope extrapolation is performed to estimate the value of endpoints $f(t_1)$ and $f(t_n)$ of sequence $f(t_i)$, $i = 1, 2, \dots, n$. An alternative is to take the average of $f(t_2)$ and $f(t_3)$ and that of $f(t_{n-2})$ and $f(t_{n-1})$ to replace $f(t_1)$ and $f(t_n)$, respectively.

To implement the algorithm practically, a few hundred repetitions of m is adequate, and the error caused by the remaining noise would less than 1% if the added noise has an amplitude that is a fraction of the standard deviation of the original data [38]. Usually, we could select a smaller number m as long as the contamination from the residue of the added noise is tolerable [57]. Considering the computation complexity and the feasibility of real-time application, we select 100 for the number m , and the outcomes are acceptable.

D. MULTI-MARGINAL HILBERT-HUANG SPECTRUM

As declared in original papers [38], [40], the Huang's decomposition method is effective in decomposing any complicated data set into a series of IMFs which permit well-behaved Hilbert transform and yield instantaneous frequencies as functions of time. The Huang's decomposition method with the Hilbert transform is called the Hilbert-Huang Transform (HHT). It has been shown in various studies that the Hilbert-Huang spectrogram (HHS) is more realistic than conventional spectrum analysis [30], [58]–[60] because no spurious harmonics or negative frequency are needed in the analysis [38], [40]. Besides, the HHT is free from the uncertainty principle's limitation to resolve more details of the signal [39], [40].

Although the spectrogram obtained from the HHT has many advantages, it may not be easy to interpret. In fact, too many details may distract the focus of our analysis from its original aim. Therefore, we introduce the multi-marginal Hilbert-Huang spectrum (MHHS) to facilitate data interpretation. The MHHS presents a measure of the total energy of each frequency of the data-trace over the entire data span. The marginal Hilbert spectrum of each IMF is

$$H(\Omega) = \int_0^T H_n(\Omega, t) dt \quad (11)$$

where $H_n(\Omega, t)$ is the Hilbert amplitude spectrum of the n^{th} IMF, Ω signifies the instantaneous frequency, and T is the time span of the IMF. In this study, we call $H(\Omega)$ mono-marginal spectrum (MMS). Accordingly, the MHHS can be defined mathematically as

$$mH(\Omega) = \sum_n \int_0^T H_n(\Omega, t) dt \quad (12)$$

where $mH(\Omega)$ is the MHHS that we need to find out. This technique is similar to the profile marginal spectrum proposed by Chen and Jeng [39] that is effective in computing the marginal spectrum of multi-dimensional data. The advantages of using MHHS are the possibility of enhancing the weak energy of some frequencies and making the whole spectrum easier to read visually.

It is important to note that the MHHS is completely different from the Fourier spectrum. In Fourier analysis, the amplitude (energy) of a given frequency Ω indicates the energy of a component of a sine or a cosine wave carried on throughout the time span of the data. In contrast, the MHHS means the accumulated energy contribution from each frequency value over the entire time span that has appeared locally in a probabilistic sense [40].

IV. MODEL STUDY

Before applying the proposed method to real EEG data, we present a synthesis example to test the algorithm's reliability by comparing the result of the proposed method with conventional technique mentioned in the previous section (III. METHODS). We opt for a Fourier-based processing scheme for the comparison, including the 60 Hz harmonic

noise muting, zero-phase finite impulse response (FIR) band-pass filtering, and Fourier spectral analysis.

Fig. 1 shows a 5 seconds synthetic model data-trace $x(t)$ with a 250 Hz sampling rate that is a combination of signal $s(t)$ and noise $n(t)$. The noise $n(t)$ is a 60 Hz harmonic wave with Gaussian white noise while the signal $s(t)$ consists of six harmonic waves of different frequencies, namely 5 Hz, 7 Hz, 9 Hz, 11 Hz, 20 Hz, and 28 Hz, with varying amplitudes.

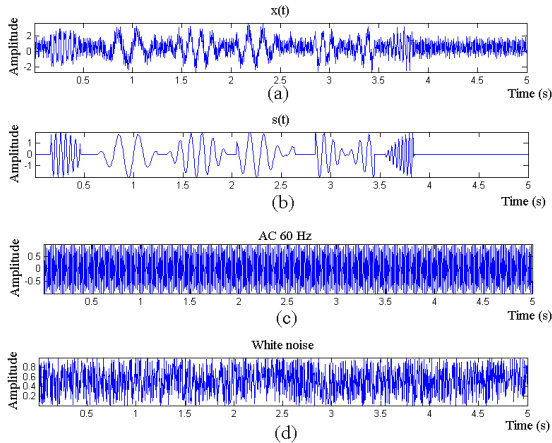


FIGURE 1. Synthetic model data. (a) Noise interfered model data-trace $x(t) = s(t) + n(t)$ where $n(t)$ comprises a 60 Hz harmonic wave with Gaussian white noise. (b) Signal $s(t)$ contains six harmonic waves of different frequencies in 4 seconds: 5 Hz, 7 Hz, 9 Hz, 11 Hz, 20 Hz, and 28 Hz. (c) AC 60 Hz harmonic noise. (d) Gaussian white noise.

The following step is to test the data analysis competence of the MHHS algorithm. The model data-trace $x(t)$ (Fig. 1a) is decomposed by using the EEMD algorithm at first, and then we select components (C2 to C8) to reconstruct the model data-trace as shown in Fig. 2a. Based on Eq. (12), the selected components are saved for generating MHHS as shown in Fig. 2b. The Fourier processing scheme is first to mute the 60 Hz AC noise with a notch filter, then a zero-phase 0.5~50 Hz band-pass FIR filter is performed to enhance the signal band. Finally, the Fourier spectrum is obtained by applying the FFT for comparison.

It can be visually discerned that the MHHS method outperforms the Fourier-based technique significantly (Fig. 2). Comparing Fig. 2a with Fig. 2c, the EEMD reconstruction successfully eliminates the baseline drift in this example. This achievement is vital because the baseline drift occurs frequently in medical data or data containing Gaussian white noise [61], [62]. Furthermore, the most important finding in the model study is that the MHHS (Fig. 2b) computed by using the proposed method exhibits much higher resolution as compared with the Fourier method, which will be shown in Section VI with real data.

V. EEG DATA ANALYSIS

The data acquired from each subject were formatted into three electrode positions, four arithmetic difficulty levels, and 25 questions on each difficulty level. Data was then read for

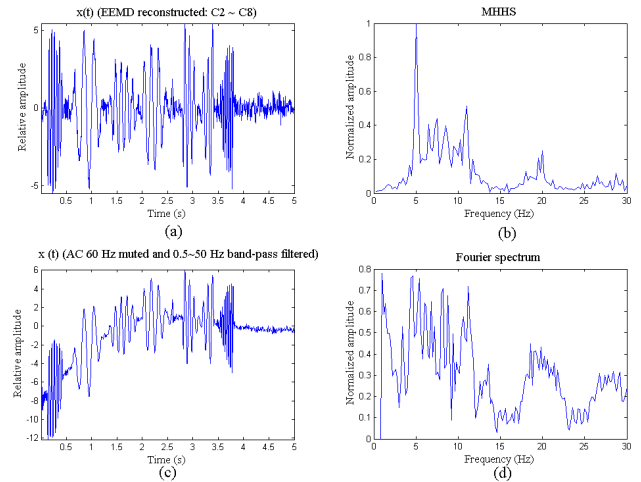


FIGURE 2. Comparison of MHHS and conventional processing scheme. (a) EEMD reconstructed data in which IMFs C2 to C8 of the model data-trace $X(t)$ are selected for reconstruction. (b) The marginal spectrum was obtained from the MHHS algorithm. (c) AC 60 Hz muted and 0.5~50 Hz band-pass filtered data in which the zero-phase FIR filter is performed. (d) Fourier spectrum of Fig. 2(c).

the frequency feature analysis to understand brain activities. Fig. 3 is a typical EEG data set acquired from subject x in this experiment with preliminary results of the proposed method. Note that the marginal spectrum shown in Fig. 3 is the MMS reflecting the energy distribution of each single IMF in the frequency domain rather than the MHHS, which will be discussed later on. As seen, the spectrum energy of raw data is dominated by the components C1 and C10, which are the high-frequency noise and background energy, respectively.

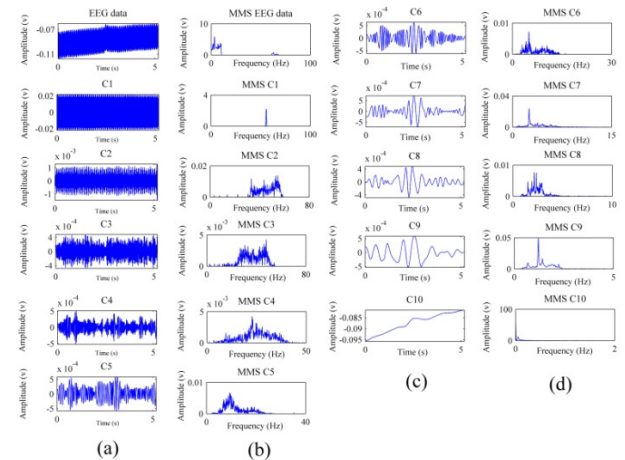


FIGURE 3. Typical EEG data acquired from subject x in this experiment. (a) Original data-trace and IMF components from C1 to C5. (b) MMS of each trace is shown in (a). (c) IMF components from C6 to C10, where C10 is the residue. (d) MMS of C6 to C10.

In this experiment, the three-electrode positions are Fpz (middle prefrontal cortex), Fp2 (right prefrontal cortex), and Fp1 (left prefrontal cortex). Dan and Reiner [7] reviewed a series of studies and concluded that frontal Theta rhythm

increases with a higher cognitive load. Holm, et al. [6] suggested that the ratio of middle frontal cortex (Fz) Theta rhythm to middle parietal cortex (Pz) Alpha rhythm is a dependable index indicating changes in the cognitive load. Our data are taken from the electrical activities of the prefrontal cortex; therefore, based on the mentioned findings, Theta rhythm is our main interest in the methodological comparison of our method with conventional technique due to its significant correlation with cognitive load.

From the feature of the energy distribution of the MMS, it is clear that Alpha rhythm resides in component C5 while Theta rhythm has its dominant energy in C6.

The complete processing scheme is briefly illustrated using a flow diagram, as shown in Fig. 4. Two cautions need to be mentioned: the NLT is optional and depends on the data quality. It applies to severely attenuated data only. In addition, the selection of using EMD or EEMD has different advantages. One should consider the computation cost and the remaining white noise interference even if the EEMD removes the mode mixing problem.

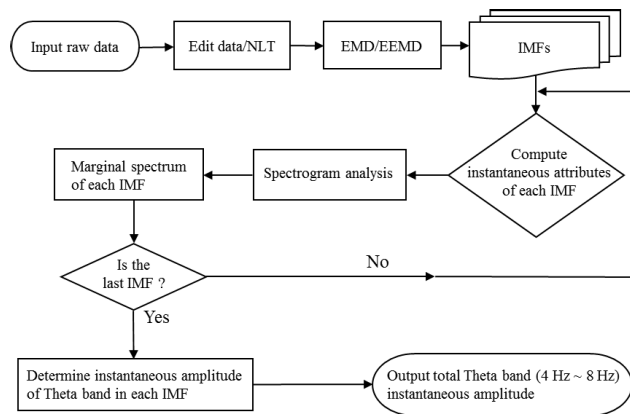


FIGURE 4. Flow diagram of the proposed method.

VI. RESULTS

A detailed comparison of our method with the Fourier based technique using data taking from a representative participant (subject x) is shown in Fig. 5 where Figs 5a, 5c, and 5e are the EEMD-MHHS derived responding Theta amplitude of individual question on each difficulty level in three positions, Fpz, Fp2, and Fp1, respectively. Figs 5b, 5d, and 5f are the corresponding performances of Fourier based technique. To make the comparison more objective, we further use the average responding Theta amplitude of 25 questions on each difficulty level to demonstrate different effects of the two methods (Figs. 5g and 5h). In general, the Theta amplitude derived from our method increases significantly with the difficulty level (Figs 5a, 5c, and 5e) while the Fourier-based technique does not, and even shows the smallest amplitude on the highest difficulty level (Figs 5b, 5d, and 5f). The unreasonable results of the Fourier-based technique are more noticeable when the average responding Theta amplitude is

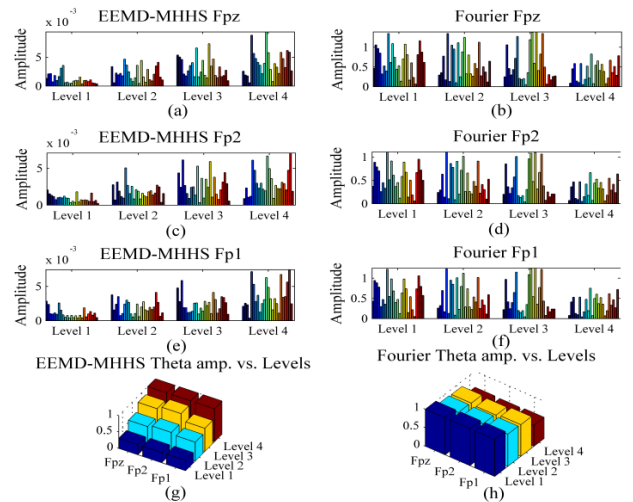


FIGURE 5. Comparison of the proposed method and Fourier based technique using data taken from subject x. The different effects of the two methods are clearly shown. (a) Responding Theta energy in Fpz was calculated by using the proposed method. (b) Responding Theta energy in Fpz was calculated by using the Fourier based technique. (c) Responding Theta energy in Fp2 was calculated by using the proposed method. (d) Responding Theta energy in Fp2 was calculated by using the Fourier based technique. (e) Responding Theta energy in Fp1 was calculated by using the proposed method. (f) Responding Theta energy in Fp1 was calculated by using the Fourier based technique. (g) Average Theta energy variation with different difficulty levels by using the proposed method. (h) Average Theta energy variation with different difficulty levels by using Fourier based technique. Bar colors in Fig. 5a to Fig. 5f indicate the number sequence of 25 questions; bar colors in Fig. 5g, and Fig. 5h denote the sequence of four different difficulty levels. The abbreviation EEMD-MHHS in the figure stands for the proposed method, while Fourier represents the Fourier based technique.

adopted, i.e. the more difficult the level, the smaller the Theta amplitude (Fig. 5h). On the contrary, our method demonstrates the significant consistency between the difficulty level and the Theta amplitude (Fig. 5g).

Some researchers may accept the results of the Fourier-based technique because similar phenomena are found in the studies of prefrontal Alpha activity [4], [63]. However, the literature review in Section III-D and our model study reveal that results derived from the Fourier based technique may be debatable.

We also provide a visual friendly illustration of results derived from the two methods (Fig. 6) to compare the Theta energy distribution in the prefrontal cortex with different levels of cognitive load tasks. The Theta energy level trend of subject x obtained from the proposed method (Fig. 6a) is opposite to that of the Fourier-based technique (Fig. 6b). An interesting outcome is the near “mirror symmetry” between these two results.

Further investigation to carry out in this study is the individual difference of 25 questions on each level. We notice that the Theta amplitude variation in 25 questions on each level (Figs. 5a-5f) has no significant trend. This could indicate the large variability of EEG energy as reported by other researchers [64]–[66]. The acceptable methodology to reach a comprehensive summary of the whole dataset is by describing

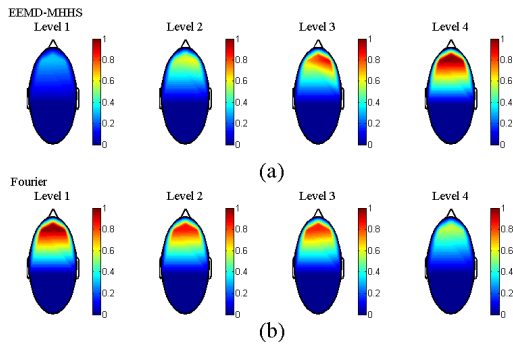


FIGURE 6. Topographic Theta energy maps of subject *x* for a quick comparison of two stated methods. (a) Results derived from the proposed EEMD-MHHS method. (b) Results derived from the Fourier based technique.

the central tendency using mean, median, or mode. Moreover, we suspect that our data may have some sort of skew due to outliers (i.e. the data distribution is not normal). Therefore, we require the median to be used as the measure of central tendency, given that the median is more robust for outliers. In this study, a quantitative comparison is achieved by employing the ANOVA (analysis of variance) test. To avoid possible bias, we add a different subject's (subject *y*) data (Figs 7c and 7d) to the analysis. The box plot shown in Fig. 7a displays the median (red mark inside the box) of the normalized amplitude of subject *x*'s Theta energy computed from the proposed EEMD-MHHS method. The top and bottom edges of the box indicate the 75th and the 25th percentiles, respectively.

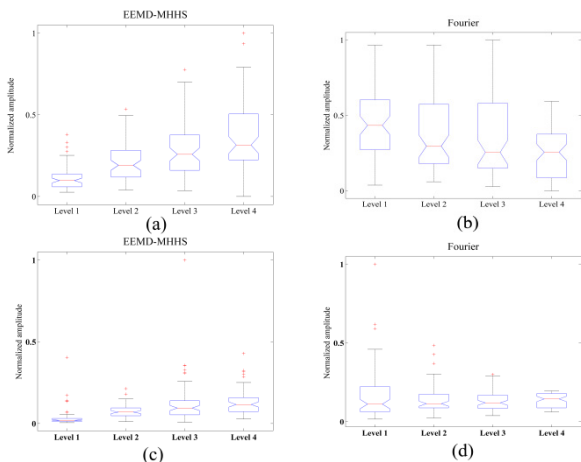


FIGURE 7. Box plot of the median of Theta amplitude on each cognitive difficulty level. (a) EEMD-MHHS results of subject *x*. (b) Fourier based technique outcomes of subject *x*. (c) EEMD-MHHS results of subject *y*. (d) Fourier based technique outcomes of subject *y*. The red mark inside the box is the median; the small red cross indicates the outlier.

The median values in Fig. 7a increase noticeably as the cognitive difficulty increases. In contrast to the proposed method, the median values obtained from the Fourier based technique generally decrease while the cognitive difficulty increases (Fig. 7b), although the trend is rather vague. Similar

outcomes are obtained from subject *y* data (Figs 7c and 7d). The outliers, appearing in Figs. 7a and 7c, imply that the data still have remaining added white noises, which result from EEMD operation. However, this phenomenon does not affect the competence of the proposed method because it can be improved greatly as long as the number of ensemble members is large enough. It should be noted that although each median displayed in the box plot is “a” given amplitude literally, it represents an amplitude composed of a series of components, each component is the amplitude of a given Theta frequency in the Theta band.

For the proposed method, the *p*-value (probability value) from the ANOVA is $8.14e-20 \leq 0.01$ (for results with a 99 percent level of confidence), and the *F*-test value is 35.9, i.e. $(F, p) = (35.9, 8.14e-20)$ for subject *x*. The further this *F*-test value deviates from 1, the more likely the underlying variances are different, suggesting that the null hypothesis may be rejected. In other words, the proposed method is effective in distinguishing Theta energy of four levels of task difficulty. Conversely, $(F, p) = (8.86, 1.21e-5)$ for the Fourier based technique, it is still effective in distinguishing Theta amplitudes of four different tasks but not as significant as the proposed method, and the “trend” is unreasonable, particularly at level 4 (Figs 7b and 7d). From the box-plots shown in Fig. 7, Theta amplitude distributions on four different levels of task difficulty vary in both methods, i.e. some are normal, and some are not. Under this condition, the ANOVA *F* test may not be sufficient. We then add the Kruskal-Wallis (*K-W*) test to the analysis. The *K-W* test is a distribution-free test and is effective when the assumptions of one-way ANOVA are not met. The calculated results of the subject *x* show that the *K-W* test value is 94.32, and the *p*-value is $2.59e-20$ for the proposed method. The Fourier based method results are 24.73 for *K-W* value and $1.75565e-5$ for *p*-value. For subject *y*, the *K-W* test value is 117.64, and the *p*-value is $2.25e-25$ for the proposed method. The Fourier based method results are 10.95 for the *K-W* test value, and 20.81 for the *p*-value. In the chi-sq table, for 4-1 degrees of freedom and alpha (the level of significance) level of 0.05, the critical chi-sq value is 7.81. For both subjects, when using the proposed method, the *K-W* test value is much higher than the critical chi-sq value while the *p*-value is extremely small, then we should reject the null hypothesis that median ranks are equal across different levels of task difficulty. Besides, the data are not necessarily normally distributed; therefore, the increasing median does not result from the increasing variance. All of the facts indicate that Theta amplitudes of four different tasks are significantly different. Compared to the proposed method, the *K-W* statistic, like the previous *F*-test, reveals that the Fourier based method is not very effective for both subjects.

To investigate how strong the relationship is between data, we calculate the correlation coefficients between the Theta amplitude and the correct answer rate, and the amplitude and the answer time (Fig. 8). In both comparisons, a strong positive correlation exists between the EEMD-MHHS derived Theta amplitude and the correct answer rate (Fig. 8a).

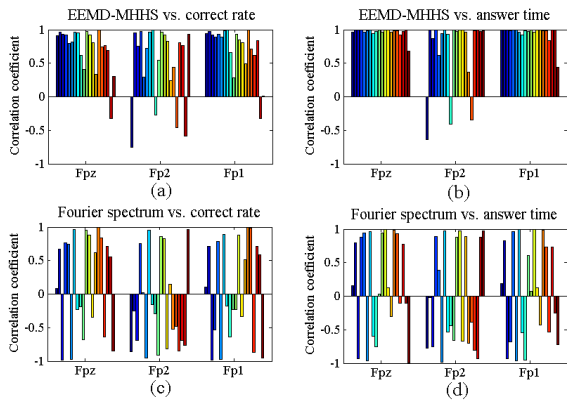


FIGURE 8. Bar charts of correlation coefficients. There are 20 bars in each electrode position, representing 20 subjects in the experiment. (a) Correlation between the EEMD-MHHS derived Theta amplitude and the correct answer rate. (b) Correlation between the EEMD-MHHS derived Theta amplitude and the answer time. (c) Correlation between the Fourier based technique derived Theta amplitude and the correct answer rate. (d) Correlation between the Fourier based technique derived Theta amplitude and the answer time.

An even stronger positive correlation is shown between the EEMD-MHHS derived Theta amplitude and the answer time (Fig. 8b). Adverse correlations are found in the results of Fourier-based technique (Figs. 8c and 8d), where about one-half of the subjects display negative correlation coefficients.

A more precise comparison between the two methods can be obtained from the same data used in Fig. 8. Table 1 shows the correlation coefficient maximal values and calculated means from that data bank.

TABLE 1. Numerical comparison of correlation coefficients.

Position	EEMD-MHHS				Fourier			
	Correct answer rate		Answer time		Correct answer rate		Answer time	
	Max.	Mean	Max.	Mean	Max.	Mean	Max.	Mean
Fpz	0.998	0.726	0.997	0.961	0.998	0.200	0.997	0.189
Fp2	0.997	0.501	0.998	0.709	0.963	-0.190	0.978	-0.040
Fp1	0.998	0.721	1.0	0.950	0.998	0.062	0.996	0.061

VII. DISCUSSION

Nowadays, the EEG has been a promising tool for the continuous and on-line measurement of cognitive load at all levels [4], [22]. With EEG’s help, instructional methods can be improved by assessing a learner’s engagement and mental load during learning tasks [7]. In educational psychology, the EEG measurement is a key technique in understanding learners’ cognitive load which indicates the total amount of mental effort being used during problem-solving, thinking, and reasoning [32]. All the above statements rely on the accurate measurement of EEG and the post-processing of the data.

We applied the EEMD in the computation to reduce the mode mixing problem, but the computation cost is high,

and it may cause artificial fluctuations in the instantaneous amplitude attribute; this is evident in the model study where one may find that the EEMD reconstructed model trace is interfered with by some noise due to the remaining white noises resulting from the EEMD algorithm. Statistically, the added white noises will not be completely removed unless the ensemble members’ number is infinite, which is impossible in practice.

In this study, we find that there is no significant difference between the results of EMD and EEMD. The possible reasons are that we do not depend too much on selecting particular IMFs with physical meaning to reconstruct data, and the mode mixing problem of our experimental EEG data is not serious. Another concern of the EMD algorithm is the orthogonality; however, it is not a necessary criterion for a non-linear decomposition like EMD [40]. Actually, in most cases, particularly when the intermittence is not a matter, the leakage due to the non-orthogonality is small.

A few studies reported that when the working memory task’s difficulty increases, the prefrontal Alpha activity decreases, whereas Theta activity increases [4], [63]. However, some investigators argued differently from the other discussions. The EEG phenomena of Alpha and Theta could vary with age, neural noise, and electrode positions [11], [67]. Although we don’t discuss the Alpha rhythm in this study, a preliminary examination of our data reveals that the Alpha rhythm seems to exhibit the same phenomenon as the Theta rhythm. In other words, it is possible that the prefrontal Alpha activity is consistent with the Theta activity. It is probably premature to take our stand on this subject, but further investigations are certainly needed. The possible correlation between Alpha and Theta rhythms reflects the complexity of the relations between cognitive load and those two brain electrical activities.

VIII. CONCLUSION

The non-linear and non-stationary data analysis is a trend in processing naturally occurring signals, including biomedical data. We introduce the EEMD-MHHS algorithm which is exactly developed from the non-linear and non-stationary system theory. The proposed method successfully resolves the connection between the signal of prefrontal electrical activity and cognitive load, particularly on the topic of Theta rhythm and cognitive load. The F-test value at 99% confidence level and the K-W test value at 95% confidence level show that the proposed method is effective in and appropriate to the EEG data processing. Besides, more significant features of the EEG signal can be extracted accurately as the MHHS algorithm is adopted. With further developments, we believe that the application of our findings will benefit the practice of learning and instruction at all levels of education.

Our results on the prefrontal Theta rhythm are generally consistent with other researchers’ findings on the frontal study. The Alpha rhythm holds some interesting topics for researching the brain’s electrical activity. Further non-linear

and non-stationary investigations on the factors in gender, age, and educational background should be decisive.

REFERENCES

- [1] F. Paas, A. Renkl, and J. Sweller, "Cognitive load theory and instructional design: Recent developments," *Educ. Psychologist*, vol. 38, no. 1, pp. 1–4, Mar. 2003.
- [2] C. W. Anderson and J. A. Bratman, "Translating thoughts into actions by finding patterns in brainwaves," in *Proc. 14th Yale Workshop Adapt. Learn. Syst.* New Haven, CT, USA: Yale Univ., 2008, pp. 1–6.
- [3] D. Ansari and D. Coch, "Bridges over troubled waters: Education and cognitive neuroscience," *Trends Cognit. Sci.*, vol. 10, no. 4, pp. 146–151, Apr. 2006.
- [4] P. D. Antonenko and D. S. Niederhauser, "The influence of leads on cognitive load and learning in a hypertext environment," *Comput. Hum. Behav.*, vol. 26, no. 2, pp. 140–150, Mar. 2010.
- [5] S. Charbonnier, R. Roy, R. Doležalová, A. Campagne, and S. Bonnet, "Estimation of working memory load using EEG connectivity measures," in *Proc. 9th Int. Joint Conf. Biomed. Eng. Syst. Technol.*, 2016, pp. 122–128.
- [6] A. Holm, K. Lukander, J. Korpela, M. Sallinen, and K. M. I. Müller, "Estimating brain load from the EEG," *Sci. World J.*, vol. 9, pp. 639–651, Jun. 2009.
- [7] A. Dan and M. Reiner, "Real time EEG based measurements of cognitive load indicates mental states during learning," *J. Educ. Data Mining*, vol. 9, no. 2, pp. 31–44, 2017.
- [8] A. Gevins, "High-resolution EEG mapping of cortical activation related to working memory: Effects of task difficulty, type of processing, and practice," *Cerebral Cortex*, vol. 7, no. 4, pp. 374–385, Jun. 1997.
- [9] J. Jin, Z. Chen, R. Xu, Y. Miao, X. Wang, and T.-P. Jung, "Developing a novel tactile P300 brain-computer interface with a cheeks-stim paradigm," *IEEE Trans. Biomed. Eng.*, vol. 67, no. 9, pp. 2585–2593, Sep. 2020.
- [10] C.-T. Lin, C.-H. Chuang, Y.-C. Hung, C.-N. Fang, D. Wu, and Y.-K. Wang, "A driving performance forecasting system based on brain dynamic state analysis using 4-D convolutional neural networks," *IEEE Trans. Cybern.*, early access, Aug. 20, 2020, doi: [10.1109/TCYB.2020.3010805](https://doi.org/10.1109/TCYB.2020.3010805).
- [11] J. Callicott, "Functional magnetic resonance imaging brain mapping in psychiatry: Methodological issues illustrated in a study of working memory in schizophrenia," *Neuropsychopharmacology*, vol. 18, no. 3, pp. 186–196, Mar. 1998.
- [12] J. M. Jansma, N. F. Ramsey, R. Coppola, and R. S. Kahn, "Specific versus nonspecific brain activity in a parametric N-Back task," *NeuroImage*, vol. 12, no. 6, pp. 688–697, Dec. 2000.
- [13] A. M. Owen, "The functional organization of working memory processes within human lateral frontal cortex: The contribution of functional neuroimaging," *Eur. J. Neurosci.*, vol. 9, no. 7, pp. 1329–1339, Jul. 1997.
- [14] A. M. Owen, K. M. Mcmillan, A. R. Laird, and E. Bullmore, "N-back working memory paradigm: A meta-analysis of normative functional neuroimaging studies," *Hum. Brain Mapping*, vol. 25, no. 1, pp. 46–59, 2005.
- [15] E. Basar, C. Basar-Eroglu, S. Karakas, and M. Schürmann, "Oscillatory brain theory: A new trend in neuroscience: The role of oscillatory processes in sensory and cognitive functions," *IEEE Eng. Med. Biol. Mag.*, vol. 18, no. 3, pp. 56–66, May 1999.
- [16] E. Başar, C. Başar-Eroglu, S. Karakas, and M. Schürmann, "Gamma, alpha, delta, and theta oscillations govern cognitive processes," *Int. J. Psychophysiol.*, vol. 39, nos. 2–3, pp. 241–248, Jan. 2001.
- [17] Y. Jeng and Y. Feng Hsiou, "Geomagnetic evidence for the time-selecting concept of traditional chinese health promotion," *IEEE Eng. Med. Biol. Mag.*, vol. 18, no. 4, pp. 94–99, 1999.
- [18] D. Mantini, M. G. Perrucci, C. Del Gratta, G. L. Romani, and M. Corbetta, "Electrophysiological signatures of resting state networks in the human brain," *Proc. Nat. Acad. Sci. USA*, vol. 104, no. 32, pp. 13170–13175, Aug. 2007.
- [19] W. Klimesch, "EEG alpha and theta oscillations reflect cognitive and memory performance: A review and analysis," *Brain Res. Rev.*, vol. 29, nos. 2–3, pp. 169–195, Apr. 1999.
- [20] W. Klimesch, B. Schack, and P. Sauseng, "The functional significance of theta and upper alpha oscillations," *Experim. Psychol.*, vol. 52, no. 2, pp. 99–108, Jan. 2005.
- [21] A. Arsalan, M. Majid, A. R. Butt, and S. M. Anwar, "Classification of perceived mental stress using a commercially available EEG headband," *IEEE J. Biomed. Health Informat.*, vol. 23, no. 6, pp. 2257–2264, Nov. 2019.
- [22] P. Zarjam, J. Epps, and F. Chen, "Spectral EEG features for evaluating cognitive load," in *Proc. Annu. Int. Conf. IEEE Eng. Med. Biol. Soc.*, Aug. 2011, pp. 3841–3844.
- [23] N. Kumar, K. Alam, and A. Hasan Siddiqi, "Wavelet transform for classification of EEG signal using SVM and ANN," *Biomed. Pharmacol. J.*, vol. 10, no. 4, pp. 2061–2069, Dec. 2017.
- [24] M. K. Mukul and F. Matsuno, "EEG de-noising based on wavelet-transforms and extraction of sub-band components related to movement imagination," in *Proc. ICROS-SICE Int. Joint Conf.*, 2009, pp. 1605–1610.
- [25] A. H. Nuttall and E. Bedrosian, "On the quadrature approximation to the Hilbert transform of modulated signals," *Proc. IEEE*, vol. 54, no. 10, pp. 1458–1459, Oct. 1966.
- [26] P. Zarjam, J. Epps, F. Chen, and N. H. Lovell, "Estimating cognitive workload using wavelet entropy-based features during an arithmetic task," *Comput. Biol. Med.*, vol. 43, no. 12, pp. 2186–2195, Dec. 2013.
- [27] V. Bajaj and R. B. Pachori, "Classification of seizure and nonseizure EEG signals using empirical mode decomposition," *IEEE Trans. Inf. Technol. Biomed.*, vol. 16, no. 6, pp. 1135–1142, Nov. 2012.
- [28] H.-T. Hsu, W.-K. Lee, K.-K. Shyu, T.-K. Yeh, C.-Y. Chang, and P.-L. Lee, "Analyses of EEG oscillatory activities during slow and fast repetitive movements using Holo-Hilbert spectral analysis," *IEEE Trans. Neural Syst. Rehabil. Eng.*, vol. 26, no. 9, pp. 1659–1668, Sep. 2018.
- [29] K.-Y. Chuang, Y.-H. Chen, P. Balachandran, W.-K. Liang, and C.-H. Juan, "Revealing the electrophysiological correlates of working memory-load effects in symmetry span task with HHT method," *Frontiers Psychol.*, vol. 10, p. 855, Apr. 2019, doi: [10.3389/fpsyg.2019.00855](https://doi.org/10.3389/fpsyg.2019.00855).
- [30] R. Shalbaf, H. Behnam, J. W. Sleight, and L. J. Voss, "Using the Hilbert-Huang transform to measure the electroencephalographic effect of propofol," *Physiological Meas.*, vol. 33, no. 2, pp. 271–285, Feb. 2012.
- [31] F. G. W. C. Paas and J. J. G. Van Merriënboer, "The efficiency of instructional conditions: An approach to combine mental effort and performance measures," *Hum. Factors, J. Hum. Factors Ergonom. Soc.*, vol. 35, no. 4, pp. 737–743, Dec. 1993.
- [32] J. Sweller, "Cognitive load during problem solving: Effects on learning," *Cognit. Sci.*, vol. 12, no. 2, pp. 257–285, Apr. 1988.
- [33] J. Sweller, J. J. G. van Merriënboer, and F. G. W. C. Pass, "Cognitive architecture and instructional design," *Educ. Psychol. Rev.*, vol. 10, no. 3, pp. 251–296, 1998.
- [34] S. J. Luck, *An Introduction to the Event-Related Potential Technique*. Cambridge, MA, USA: MIT Press, 2005.
- [35] G. Buzsáki, *Rhythms of the Brain*. Oxford, U.K.: Oxford Scholarship, 2006.
- [36] T. Hinault and P. Lemaire, "What does EEG tell us about arithmetic strategies? A review," *Int. J. Psychophysiology*, vol. 106, pp. 115–126, Aug. 2016.
- [37] C.-S. Chen and Y. Jeng, "Natural logarithm transformed EEMD instantaneous attributes of reflection data," *J. Appl. Geophys.*, vol. 95, pp. 53–65, Aug. 2013.
- [38] Z. Wu and N. E. Huang, "Ensemble empirical mode decomposition: A noise-assisted data analysis method," *Adv. Adapt. Data Anal.*, vol. 1, no. 1, pp. 1–41, Jan. 2009.
- [39] C.-S. Chen and Y. Jeng, "GPR investigation of the near-surface geology in a geothermal river valley using contemporary data decomposition techniques with forward simulation modeling," *Geothermics*, vol. 64, pp. 439–454, Nov. 2016.
- [40] N. E. Huang, Z. Shen, S. R. Long, M. L. Wu, H. H. Shih, Q. Zheng, N. C. Yen, C. C. Tung, and H. H. Liu, "The empirical mode decomposition and the Hubert spectrum for nonlinear and non-stationary time series analysis," *Proc. Roy. Soc. A, Math., Phys. Eng. Sci.*, vol. 454, no. 1971, pp. 903–995, 1998.
- [41] D. Wechsler, *Wechsler Adult Intelligence Scale*, 3rd ed. San Antonio, TX, USA: Psychol. Corp., 1997.
- [42] C. M. Sweeney-Reed, S. J. Nasuto, M. F. Vieira, and A. O. Andrade, "Empirical mode decomposition and its extensions applied to EEG analysis: A review," *Adv. Data Sci. Adapt. Anal.*, vol. 10, pp. 1–35, Apr. 2018.
- [43] P. Flandrin, G. Rilling, and P. Goncalves, "Empirical mode decomposition as a filter bank," *IEEE Signal Process. Lett.*, vol. 11, no. 2, pp. 112–114, Feb. 2004.
- [44] C.-S. Chen and Y. Jeng, "A data-driven multidimensional signal-noise decomposition approach for GPR data processing," *Comput. Geosci.*, vol. 85, pp. 164–174, Dec. 2015.
- [45] K. Gröchenig, *Foundations of Time-Frequency Analysis: Applied and Numerical Harmonic Analysis*. Boston, MA, USA: Birkhäuser, 2001.

- [46] N. E. Huang and S. S. P. A. Shen, *Hilbert-Huang Transform and Its Applications*. Singapore: World Scientific, 2005.
- [47] N. E. Huang and Z. Wu, "A review on Hilbert-Huang transform: Method and its applications to geophysical studies," *Rev. Geophys.*, vol. 46, no. 2, pp. 1–23, 2008, Art. no. RG2006.
- [48] J. S. Bendat and A. G. Piersol, *Random Data: Analysis and Measurement Procedures*, 4th ed. New York, NY, USA: Wiley, 2012.
- [49] L. Cohen, *Time-Frequency Analysis: Theory and Applications*. Englewood Cliffs, NJ, USA: Prentice-Hall, 1995.
- [50] D. Gabor, "Theory of communication," *J. Inst. Elect. Eng.*, vol. 93, no. 26, pp. 429–441, Nov. 1946.
- [51] N. Anstey, "Attributes in color: The early years," *CSEG Recorder*, vol. 30, no. 3, pp. 12–15, 2005.
- [52] A. E. Barnes, "A tutorial on complex seismic trace analysis," *Geophysics*, vol. 72, no. 6, pp. W33–W43, Nov. 2007.
- [53] M. T. Taner, F. Koehler, and R. E. Sheriff, "Complex seismic trace analysis," *Geophysics*, vol. 44, no. 6, pp. 1041–1063, Jun. 1979.
- [54] Y. Zhou, W. Chen, J. Gao, and Y. He, "Application of Hilbert–Huang transform based instantaneous frequency to seismic reflection data," *J. Appl. Geophys.*, vol. 82, pp. 68–74, Jul. 2012.
- [55] N. E. Huang, Z. Wu, S. R. Long, K. C. Arnold, X. Chen, and K. Blank, "On instantaneous frequency," *Adv. Adapt. Data Anal.*, vol. 1, no. 2, pp. 177–229, Apr. 2009.
- [56] C.-S. Chen and Y. Jeng, "Nonlinear data processing method for the signal enhancement of GPR data," *J. Appl. Geophys.*, vol. 75, no. 1, pp. 113–123, Sep. 2011.
- [57] Z. Wu, N. E. Huang, and X. Chen, "The multi-dimensional ensemble empirical mode decomposition method," *Adv. Adapt. Data Anal.*, vol. 1, no. 3, pp. 339–372, 2009.
- [58] J. Han and M. van der Baan, "Empirical mode decomposition for seismic time-frequency analysis," *Geophysics*, vol. 78, no. 2, pp. 9–19, Mar. 2013.
- [59] Y. Jeng, M.-J. Lin, C.-S. Chen, and Y.-H. Wang, "Noise reduction and data recovery for a VLF-EM survey using a nonlinear decomposition method," *Geophysics*, vol. 72, no. 5, pp. F223–F235, Sep. 2007.
- [60] R. J. Oweis and E. W. Abdulhay, "Seizure classification in EEG signals utilizing Hilbert-huang transform," *Biomed. Eng. OnLine*, vol. 10, no. 1, p. 38, 2011, doi: 10.1186/1475-925X-10-38.
- [61] H. Zhang, "An improved QRS wave group detection algorithm and MATLAB implementation," *Phys. Procedia*, vol. 25, pp. 1010–1016, Jan. 2012.
- [62] H. Beyramianlou and N. Lotfivand, "Shannon's energy based algorithm in ECG signal processing," *Comput. Math. Methods Med.*, vol. 2017, pp. 1–16, Jan. 2017.
- [63] A. Gevins, "Neurophysiological measures of working memory and individual differences in cognitive ability and cognitive style," *Cerebral Cortex*, vol. 10, no. 9, pp. 829–839, Sep. 2000.
- [64] L. Cummings, A. Dane, J. Rhodes, P. Lynch, and A. M. Hughes, "Diurnal variation in the quantitative EEG in healthy adult volunteers," *Brit. J. Clin. Pharmacol.*, vol. 50, no. 1, pp. 21–26, Jul. 2000.
- [65] A. Kondacs and M. Szabó, "Long-term intra-individual variability of the background EEG in normals," *Clin. Neurophysiol.*, vol. 110, no. 10, pp. 1708–1716, Oct. 1999.
- [66] V. E. Pollock, L. S. Schneider, and S. A. Lyness, "Reliability of topographic quantitative EEG amplitude in healthy late-middle-aged and elderly subjects," *Electroencephalogr. Clin. Neurophysiol.*, vol. 79, no. 1, pp. 20–26, Jul. 1991.
- [67] B. Schack, W. Klimesch, and P. Sauseng, "Phase synchronization between theta and upper alpha oscillations in a working memory task," *Int. J. Psychophysiol.*, vol. 57, no. 2, pp. 105–114, Aug. 2005.



CHIH-SUNG CHEN received the Ph.D. degree in earth sciences from National Taiwan Normal University, in 2011. He is currently a Postdoctoral Research Associate of systems and biomedical engineering with the Department of Electrical Engineering, National Central University, Taiwan. He has worked on investigations of the time series analysis applied to geosciences over the past ten years using a range of nonlinear and nonstationary workflows. His research interests include geophysics, time-frequency-amplitude processing, multimodal signal processing, multimodal big data analytics, and development of intelligent systems. In 2017, he received the Postdoctoral Academic Publication Award from the Ministry of Science and Technology, Taiwan.



TSUNGH-SIN CHIEN received the M.S. degree from National Taiwan Normal University, Taiwan, in 2017. His research interests include science education, signal processing, EEG-based brain-computer interface design, and biomedical circuits.



PO-LEI LEE (Member, IEEE) was born in 1973. He received the B.S. degree in electrical engineering from National Cheng-Kung University, Taiwan, in 1995, and the Ph.D. degree from the Institute of Biomedical Engineering, National Yang-Ming University, Taiwan, in 2000. From 2001 to 2005, he was a Postdoctoral Fellow with the Taipei Veterans General Hospital, researching the signal and image-analysis procedures for electroencephalography and magnetoencephalography signals. He joined the Department of Electrical Engineering, National Central University, Taiwan, in 2005. His research interests include signal and image processing of EEG and MEG signals and designing the EEG-based brain-computer interfaces.



YIH JENG (Member, IEEE) received the B.S. degree in physics (five years B.S. program) from National Taiwan Normal University, in 1976, the M.S. degree in geophysics from National Central University, Taiwan, R.O.C., in 1978, and the Ph.D. degree in geophysics from the University of Connecticut, in 1986. From 1986 to 1988, he was a Postdoctoral Research Associate with the University of Connecticut. He joined the Department of Earth Sciences, National Taiwan Normal University, in 1988, and became a Geophysics Professor in 1992. He has been awarded the distinguished professorship two times since 2014. His research interests include near-surface geophysics, archaeological prospecting, and nonlinear time-frequency analysis. His research interests also include martial arts, chi-kong, and geomagnetic effect on brain waves. He was a Trustee of BIOEM and CGS and a member of NSG and SEG. He is also an Emeritus Lifetime member of EGU. He received 43 research grants and 18 P.I. honorarium awards from 1989 to 2016. He retired as a Distinguished Professor in 2017.



TING-KUANG YEH received the Ph.D. degree from National Taiwan Normal University. He is currently an Associate Professor with the Institute of Marine Environmental Science and Technology/Science Education Center, National Taiwan Normal University. His research interests include integrating genomics, neuroscience, and cognitive science into educational practices. His research work has been focused on the following two series: investigating learning mechanisms, putting such a mechanism into adaptive instruction, and the implication/application of adaptive instruction in various disciplinary topics.

• • •